

Excitonic effects in optical absorption and electron-energy loss spectra of hexagonal boron nitride

Ludger Wirtz,¹ Andrea Marini,² Myrta Grüning,³ and Angel Rubio^{3,4,5}

¹*Institute for Electronics, Microelectronics, and Nanotechnology (IEMN), CNRS-UMR 8520, B.P. 60069, 59652 Villeneuve d'Ascq Cedex, France*

²*Istituto Nazionale per la Fisica della Materia e Dipartimento di Fisica dell'Università di Roma "Tor Vergata", Via della Ricerca Scientifica, I-00133 Roma, Italy*

³*Donostia International Physics Center (DIPC), 20018 Donostia-San Sebastián, Spain*

⁴*Department of Material Physics, UPV/EHU and Centro Mixto CSIC-UPV, 20018 San Sebastián, Spain*

⁵*Institut für Theoretische Physik, Freie Universität Berlin, Arnimallee 14, D-14195 Berlin, Germany*

(Dated: February 2, 2008)

A new interpretation of the optical and energy-loss spectra of hexagonal boron nitride is provided based on first-principle calculations. We show that both spectra cannot be explained by independent-particle transitions but are strongly dominated by excitonic effects. The lowest direct and indirect gaps are much larger than previously reported. The direct gap amounts to 6.8 eV. The first absorption peak at 6.1 eV is due to an exciton with a binding energy of 0.7 eV. We show that this strongly bound Frenkel exciton is also responsible for the low frequency shoulder of the π plasmon in the energy-loss function. Implications for nanotube studies are discussed.

PACS numbers: 78.20.-e, 71.35.Cc, 71.45.Gm

Hexagonal boron nitride (hBN) is isoelectronic to graphite and has a similar layered structure. Recently, the electronic structure and the optical properties of hBN have regained interest due to the discovery of BN-nanotubes^{1,2} which can be considered as cylinders formed by rolling a single sheet of hBN onto itself. While graphite is a semi-metal with a linear crossing of the π and π^* bands at the K-point, in hBN the different electronegativities of boron and nitrogen lift the degeneracy at the K-point and lead to a large gap. It was predicted³ that hBN has an indirect quasi-particle gap of 5.4 eV and a minimum direct quasi-particle gap of 6.2 eV. Measurements of the optical absorption coefficient^{4,5,6,7,8} yield unanimously an absorption peak with a maximum between 6.1 and 6.2 eV. The spectra in these papers are interpreted in terms of independent electron transitions from the valence to the conduction band. The onset of the absorption peak (varying in the different experiments between 5.2 and 5.5 eV) is consequently considered to be a measure of the band gap. However, calculations⁹ at the Random Phase Approximation (RPA) level, i.e., in the picture of independent electron excitations, yield spectra whose shape is not in good agreement with the experimental spectra. Furthermore, in a recent luminescence experiment¹⁰, evidence for a direct bandgap at 5.97 eV and a series of bound excitons with a maximum binding energy of 0.149 eV was found. In this communication, we reinterpret the different experimental results and demonstrate the importance of excitonic effects for a proper understanding of both absorption and electron-loss spectra.

For the interpretation of the spectra, we calculate the real and imaginary parts, $\epsilon_1(E)$ and $\epsilon_2(E)$, of the energy-dependent macroscopic dielectric function on two levels of approximation: i.) using RPA, ii) on the GW+BS level, i.e., including quasi-particle corrections on the level of the GW-method and calculating excitonic effects

through the Bethe-Salpeter (BS) equation¹¹. In both cases, we start with a calculation of the wavefunctions using density-functional theory (DFT). With the code ABINIT¹² we calculate¹³ the valence-band wavefunctions and a large number of conduction-band states, ψ_{nk} , with a band-index n and a sufficiently fine sampling of the crystal momentum \mathbf{k} . In this work we use two descriptions of exchange-correlation effects: the customary local density approximation (LDA) and the exact-exchange (EXX) potential. To obtain the EXX potential we followed Ref. 14.

On the level of the RPA (which corresponds to the use of Fermi's golden rule for $\epsilon_2(E)$), we compute the optical spectra in terms of the dipole-matrix averaged joint-density-of-states. However, ground-state DFT provides only a qualitative and, often incorrect, description of the excited states. The reason is that many-body effects beyond the independent particle approximation are neglected. But in systems with a poor electronic screening, the electron-hole attraction can be far from negligible. Good agreement with experiments is restored by using the self-energy approach of many body perturbation theory¹¹. Starting from the DFT energies and wavefunctions, we calculate the quasi-particle energies ("true" single-particle excitation energies), E_{nk} , by solving the Dyson equation:

$$\left[-\frac{\nabla^2}{2} + V_{ext} + V_{Hartree} + \Sigma(E_{nk}^{qp}) \right] \psi_{nk}^{qp} = E_{nk}^{qp} \psi_{nk}^{qp}. \quad (0.1)$$

The self-energy Σ is approximated as the energy convolution of the one-particle Green's function G and the (RPA) dynamically screened Coulomb interaction W , ($\Sigma = iGW$). We perform a "semi-self consistent" (GW₀) calculation by updating the quasi-particle energies in G (but not in W) until the resulting quasi-particle ener-

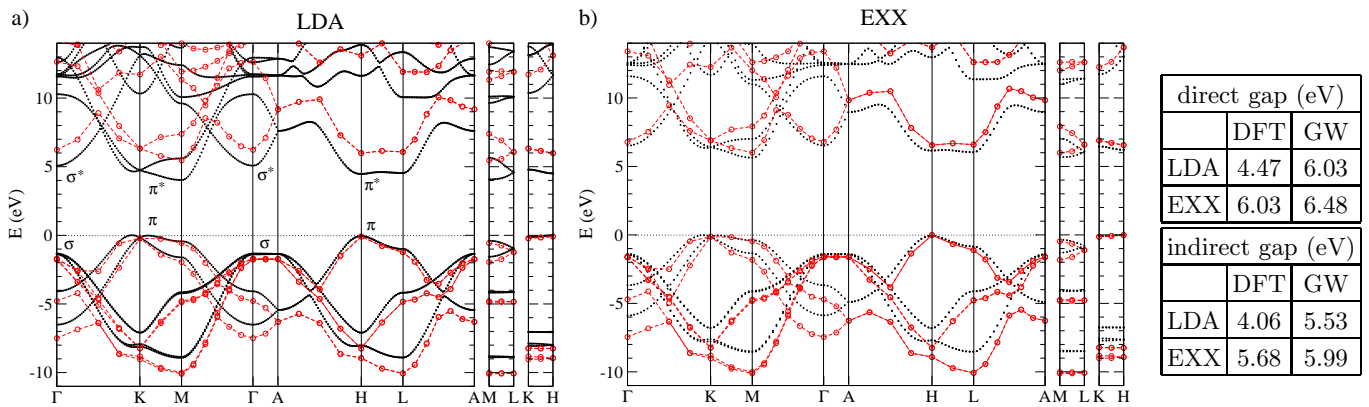


FIG. 1: Bandstructure of hBN: a) LDA (dotted lines), LDA-GW (circles); b) EXX (dotted lines), EXX-GW (circles). Right panel: summary of the direct and indirect gap for hBN in the different approximations of panels a) and b).

gies are converged. This procedure yields a quasi-particle bandgap for hBN that is about 0.3 eV higher than the one obtained on the non-self consistent (G_0W_0) level. In order to assess how important are the initial eigenfunctions in this procedure, we performed calculations starting from LDA or EXX states.

Electron-hole attraction (excitonic effects) is included by solving the Bethe-Salpeter equation¹¹

$$(E_{c\mathbf{k}}^{qp} - E_{v\mathbf{k}}^{qp})A_{v\mathbf{c}\mathbf{k}}^S + \sum_{\mathbf{k}'v'c'} \langle v\mathbf{c}\mathbf{k} | K_{eh} | v'\mathbf{c}'\mathbf{k}' \rangle A_{v'\mathbf{c}'\mathbf{k}'}^S = \Omega^S A_{v\mathbf{c}\mathbf{k}}^S. \quad (0.2)$$

$A_{v\mathbf{c}\mathbf{k}}^S$ are the excitonic eigenstate projections onto the electron-hole basis. The interaction kernel K_{eh} “mixes” different electron transitions from valence band states v, v' to conduction band states c, c' leading to modified transition energies Ω^S . The overall effect in the spectra is a redistribution of oscillator strength as well as the appearance of new-states within the bandgap (bound excitons). The GW+BS calculations are performed with the code SELF¹⁸.

In Fig. 1, we present the bandstructure of hBN obtained using the LDA and EXX approximations and compare with the GW-calculation. On the LDA and GW levels, we reproduce quite accurately the results of Ref. 3. The GW-correction increases the direct bandgap (at the M-point) by 1.56 eV. Fig. 1 also includes the values for the direct and indirect gaps¹⁵. The bare EXX bandstructure resembles very closely the LDA GW-bandstructure. The GW-correction on top of EXX wave-functions yields an additional increase of the direct bandgap of 0.45 eV. However it still underestimates the “true” direct bandgap that must be close to 6.8 eV in order to describe the measured optical spectra (see below).

Our results for the energy-dependent dielectric function of hBN (light polarization parallel to the layers) are shown in Fig. 2 and compared with the experimental data of Ref. 6. The experimental ϵ_1 and ϵ_2 were extracted from the electron-energy loss function through a Kramers-Kronig analysis⁶. Since the experimental broadening is about 0.2 eV, we use the same value in our calculations. In Fig. 2 a) we present calcu-

lations based on LDA-wavefunctions. The dash-dotted line shows the RPA absorption spectrum (in agreement with earlier RPA calculations⁹). The broad peak with a maximum at 5.6 eV is entirely due to the continuum of inter-band transitions between the π and π^* bands (see Fig. 1). The calculated GW+BS absorption spectrum displays a double peak structure with the main peak at 5.45 eV and a second peak at 6.15 eV. The nature of the spectrum is entirely different from the RPA spectrum: the first peak is due to a strongly bound exciton, and the second peak contains contributions from higher excitons and from the onset of the continuum of inter-band transitions (see below). The similarity between the RPA and GW+BS spectra stems exclusively from the strong broadening employed in the calculation. The main peaks in the two spectra are at about the same position because of an almost-cancellation between the bandgap widening due to the GW-approximation and the red-shift of oscillator strength due to excitonic effects. Comparison with Fig. 2 b) shows that the shape of the GW+BS spectrum is in much better agreement with experiment than the RPA spectrum. This underlines the importance of excitonic effects in hBN. The influence of excitonic effects becomes even more pronounced when we compare the real part of ϵ . Only the GW+BS calculation can reproduce qualitatively the shape of the experimental ϵ_1 .

While the shape of the experimental spectrum is well reproduced by the LDA GW+BS calculation, the absolute position is not: The main peak in the experiment is 0.65 eV higher than in the LDA GW+BS spectrum. We suppose that the quasi-particle gap is higher than the one predicted by the LDA GW method. In order to check this hypothesis, we performed calculations based on EXX wave-functions. In Fig. 1 we showed that the EXX GW gap is wider by 0.45 eV than the LDA GW gap. This is manifested in Fig. 2 c) where the absorption spectrum having similar shape to the LDA GW+BS one is blue-shifted by 0.45 eV¹⁹. The remaining difference of 0.2 eV with respect to the experimental spectrum is most likely due to a short-coming of the GW-approximation (pos-

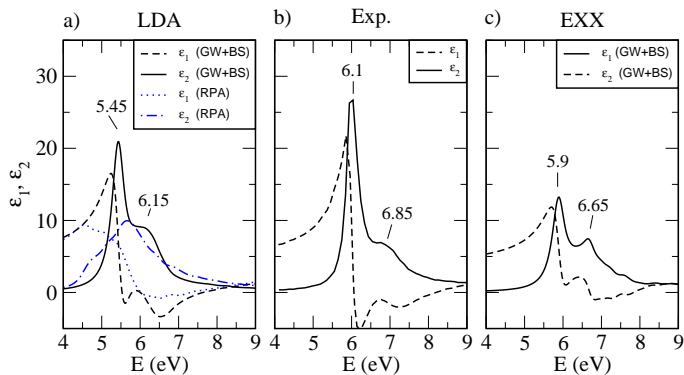


FIG. 2: Real (ϵ_1) and imaginary (ϵ_2) parts of the dielectric function of hBN calculated using LDA (a) or EXX (c). The experimental data from Ref. 6 is shown in (b). For the LDA results in a) we add the comparison with the results obtained at the RPA and full GW+BS levels. The calculations include a Lorentzian broadening of 0.2 eV (full-width at half-maximum). The light-polarization is parallel to the BN layers.

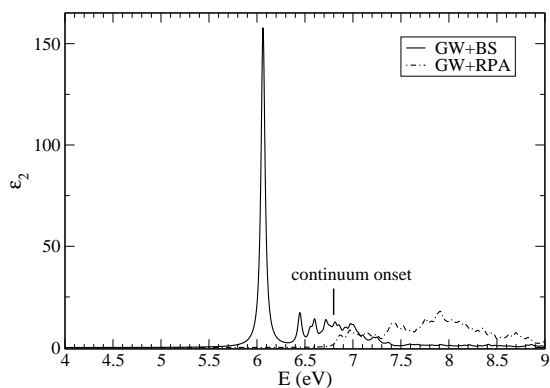


FIG. 3: Absorption spectrum of hBN calculated with a Lorentzian broadening of 0.025 eV. Solid line: LDA GW+BS calculation (with additional scissor operator - see text). Dotted line: LDA GW RPA.

sibly due to the neglect of vertex corrections). In what follows we will present calculations based on LDA wavefunction and energies. Beyond the GW-correction, we will introduce an additional scissor (0.65 eV) with a value such that the first absorption peak at 6.1 eV, in agreement with experiments^{4,5,6,7} is properly reproduced.

In Fig. 3 we show the “shifted” GW+BS spectrum with a broadening of 0.025 eV. We also display the GW RPA spectrum (corresponding to independent quasi-particle transitions). The onset of the latter at 6.8 eV marks the direct quasi-particle gap with respect to which the exciton binding energy is calculated. There is a sequence of bound excitonic peaks below the onset of the continuum. Most of the oscillator strength is collected by the first bound exciton which is doubly degenerate and has a binding energy of 0.7 eV. Upon broadening, the higher bound excitons and the absorption at the continuum edge form together the second peak at 6.85 eV which has been

singlet excitons	triplet excitons
6.365 eV	6.365 eV
6.291 eV	6.192 eV
6.100 eV	6.031 eV
6.028 eV	5.941 eV

FIG. 4: Energy scheme of optically active (solid line) and “dark” (dashed lines) excitonic states around the first absorption peak at 6.1 eV.

observed in experiments^{5,6} and can be seen in Fig. 2. Our results are therefore in good agreement with the experimental data. It is also in good agreement with the recent optical absorption measurement in ref. 7, assuming that their absorption peak at 6.1 eV is strongly broadened due to sample quality of experimental resolution. However, the interpretation of the experiments has changed: While up to now, the spectrum of hBN has always been interpreted in terms of a *continuum of inter-band transitions* with a *direct gap between 5.4 and 5.8 eV*, our calculations show that the spectrum is dominated by a *strongly bound discrete Frenkel excitons with a direct quasi-particle gap of 6.8 eV*.

Recently, Watanabe et al.¹⁰ presented optical absorption data that is seemingly in contradiction with previous experimental data and with our theoretical results. They find evidence for a direct bandgap of 5.971 eV with a series of four bound excitons at 5.822, 5.945, 5.962, and 5.968 eV. The binding energy of the first exciton is therefore 0.149 eV in stark contrast with our value of 0.7 eV. However, the absorption data of Ref. 10 stops at 6 eV, making a comparison with previous absorption data difficult. We suggest that the peaks that they observe are due to the excitation of “dark” excitons, i.e., excitonic states that are forbidden by the dipole selection rules but that might be accessible when the symmetry of the crystal is broken through defects or limited sample quality or when spin-orbit interaction is strong enough to lead to spin-flip (i.e., excitation of triplet-excitons via intersystem crossing). In Fig. 4, we present schematically the levels of all active and dark excitons in the energy range around the first optically allowed exciton at 6.1 eV. At 0.072 eV below this value a dark singlet exciton is found, and at 0.159 and 0.069 eV below the first optically allowed singlet exciton, two triplet excitons are found. These energy values do not correspond exactly to the absorption peaks of Ref. 10, but they may explain qualitatively the occurrence of additional absorption peaks below 6.1 eV in the work of ref. 10. The limited accuracy of the approximations used in the calculations together with the possible role of exciton-phonon coupling could explain the remaining discrepancies. We note that our calculations are at variance with the calculations of Ref. 16 that argue that the first absorption peak is composed of 4 different optically active excitons.

Another important check of interpretation is the di-

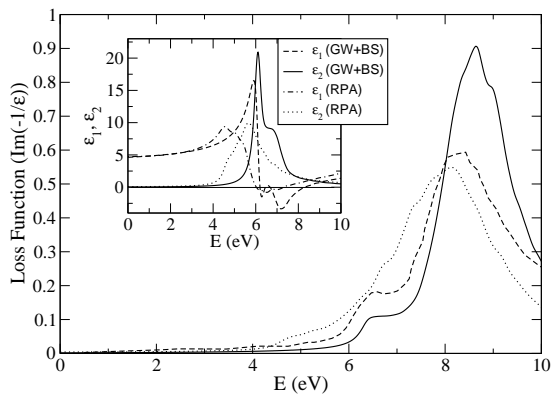


FIG. 5: Calculated loss function of hBN within the RPA (dotted line) and GW+BS (full-line). Dashed line: experimental loss function of ref. 6. Inset: Real and imaginary part the dielectric function in the GW+BS and RPA methods.

rect comparison between calculated and measured loss-function of hBN⁶. This is done in Fig. 5 where we compare the RPA and GW+BS results. The experimental loss function displays a peak around 8.4 eV which is due to plasma-oscillations of the π -electrons. It has a shoulder at 6.5 eV which has never been explained. A similar shoulder has been recently observed in the electron-energy loss spectra of multi-wall BN nanotubes²⁰. Inspecting the real part of the calculated dielectric function, ϵ_1 , in the inset of Fig. 5, the origin of this shoulder

becomes clear. A peak in the loss function occurs close to the energies where ϵ_1 changes its sign from negative to positive. While the RPA-calculation yields only one such crossing and consequently only one plasmon peak, the excitonic effects lead to an additional crossing at 6.5 eV which causes the shoulder of the π -plasmon peak, in perfect agreement with experiments.

In conclusion, we have proposed a new scenario to explain the spectroscopic properties of hBN. The main absorption peak of hBN at 6.1 eV is due to a strongly bound exciton with a binding energy of 0.7 eV. This means that the “true” minimum direct quasi-particle gap is 6.8 eV which is considerably larger than predicted previously³. The additional “excitonic” peaks observed in Ref. 10 can be explained as due to a relaxation of the selection-rules due to symmetry breaking and/or due to spin-flip (singlet to triplet interconversion). We also show that the electron-energy loss spectra of hBN show a characteristic influence of excitonic effects that manifest itself as a shoulder at lower energies of the main π -plasmon peak. We expect that these excitonic effects will also play an important role in the interpretation of experiments on EELS of isolated BN-nanotubes⁸.

The work was supported by the EU network of excellence NANOQUANTA (NMP4-CT-2004-500198) and the French GDR “nanotubes”. Calculations were performed at IDRIS (Project No. 51827) and CEPBA. A.R. acknowledges the Humboldt Foundation under the Bessel research award (2005),

- ¹ A. Rubio, J. L. Corkill, and M. L. Cohen, Phys. Rev. B **49**, R5081 (1994); X. Blase, A. Rubio, S. G. Louie, and M. L. Cohen, Europhys. Lett **28**, 335 (1994).
- ² N. G. Chopra, J. Luyken, K. Cherry, V. H. Crespi, M. L. Cohen, S. G. Louie, and A. Zettl, Science **269**, 966 (1995).
- ³ X. Blase, A. Rubio, S.G. Louie and M. L. Cohen, Phys. Rev. B **51**, 6868 (1995)
- ⁴ A. Zunger, A. Katzir, and A. Halperin, Phys. Rev. B **13**, 5560 (1976).
- ⁵ D. M. Hoffman, G. L. Doll, and P. C. Eklund, Phys. Rev. B **30**, 6051 (1984).
- ⁶ C. Tarrío and S. E. Schnatterly, Phys. Rev. B **40**, 7852 (1989).
- ⁷ J. S. Lauret, R. Arenal, F. Ducastelle, A. Loiseau, M. Cau, B. Attal-Tretout, and E. Rosencher, Phys. Rev. Lett. **94**, 037405 (2005).
- ⁸ R. Arenal, O. Stéphan, m. Kociak, D. Taverna, A. Loiseau, and C. Colliex, submitted (2005).
- ⁹ Y. N. Xu and W. Y. Ching, Phys. Rev. B **44**, 7787 (1991). G. Cappellini, G. Satta, M. Palummo, and G. Onida, Phys. Rev. B **64**, 035104 (2001); A. G. Marinopoulos, L. Wirtz, A. Marini, V. Olevano, A. Rubio, and L. Reining, Appl. Phys. A **78**, 1157 (2004); G.Y. Guo and J.C. Lin, Phys. Rev. B **71**, 165402 (2005).
- ¹⁰ K. Watanabe, T. Taniguchi, and H. Kanda, Nature Materials **3**, 404 (2004).
- ¹¹ See, e.g., G. Onida, L. Reining, and A. Rubio, Rev. Mod. Phys. **74**, 601 (2002).
- ¹² X. Gonze, J.-M. Beuken, R. Caracas, F. Detraux, M. Fuchs, G.-M. Rignanese, L. Sindic, M. Verstraete, G. Zerah, F. Jollet, M. Torrent, A. Roy, M. Mikami, Ph. Ghosez, J.-Y. Raty, D.C. Allan, Comp. Mat. Sci. **25**, 478 (2002).
- ¹³ Core electrons are substituted by Trouillier-Martins pseudo-potentials in the Kleinman-Bylander form with a cutoff radius of 1.59 a.u. for B and 1.50 a.u. for N. Wave functions are expanded in plane waves with an energy cut-off at 30 Hartree. With these parameters, geometry optimization leads to a bond-length of 1.441 Å and an inter-sheet distance of 3.251 Å. For the calculation of the dielectric function $\epsilon(E)$ we used conduction band states with energies up to 70 eV above the highest valence band state (corresponding to $n = 50$ bands). Crystal-local field effects are included through the off-diagonal elements of the dielectric matrix $\epsilon_{\mathbf{G},\mathbf{G}'}(E)$ in reciprocal space. We use 50 G-vectors. The convergence of the final spectra with all parameters was carefully checked. For the GW-calculations we use a $12 \times 12 \times 4$ Monkhorst-Pack k-point sampling of the 1st Brillouin-zone (leading to convergence to within 0.05 eV) The grid is not shifted (i.e., the Γ -point is included). For the BS calculations we use a $24 \times 24 \times 10$ k-point grid (leading to full convergence of the first and second excitonic peaks - the higher order bound excitons in Fig. 3 are susceptible to small changes for finer k-point grids).
- ¹⁴ M. Städele, J. A. Majewski, P. Vogl, and A. Görling, Phys. Rev. Lett. **79**, 2089 (1997). We solved the equations em-

ploying LDA wavefunctions as basis set. We used bands upto 170 eV (200 bands) to determine the EXX potential, 287 reciprocal lattice vectors and a $8 \times 8 \times 2$ k-point grid (shifted 0.0,0.0,0.5). The Bandgap is converged to 0.05 eV. LDA correlation is added on top of the EXX potential.

¹⁵ There is a discrepancy with a recent all-electron GW calculation¹⁶ which reports a direct LDA GW-band gap of 6.47 and an indirect gap of 5.95. The difference can possibly be traced back to the fact that their in-plane static dielectric constant is only 4.40 while we obtain 4.71 which is closer to the experimental value of 4.95 eV¹⁷.

¹⁶ B. Arnaud, S. Lebègue, P. Rabiller, and M. Alouani, cond-mat/0503390.

¹⁷ R. Geick, C. H. Perry, and G. Rupprecht, Phys. Rev. **146**, 543 (1966).

¹⁸ SELF, (<http://people.roma2.infn.it/~marini/self/>) written by A. Marini

¹⁹ As a consequence of the large EXX-band gap, the static dielectric constant, $\epsilon_0 = 4.4$, calculated in EXX-RPA strongly underestimates the experimental value of 4.95¹⁷. This leads to an overestimation of the excitonic binding energy. However, the resulting value of the BS+GW calculation, $\epsilon_0 = 4.7$, is larger than the EXX-RPA RPA value and close to the LDA-RPA value. In principle, one should perform BS-calculations with the updated screening until self-consistence is reached. Since this is computationally too expensive, we decided to take the LDA-RPA screening (which is sufficiently close to the experimental one) in combination with the EXX wavefunctions and energies.

²⁰ G. G. Fuentes, E. Borowiak-Palen, T. Pichler, X. Liu, A. Graff, G. Behr, R. J. Kalenczuk, M. Knupfer, and J. Fink, Phys. Rev. B **67**, 035429 (2003).